JOC Article

# Design of New Bidentate Ligands Constructed of Two Hoechst 33258 Units for Discrimination of the Length of Two $A_3T_3$ Binding Motifs

Mikimasa Tanada, Saori Tsujita, and Shigeki Sasaki*

*Graduate School of Pharmaceutical Sciences, Kyushu University, 3-1-1 Maidashi, Higashi-ku, Fukuoka 812-8582, Japan*

*sasaki@phar.kyushu-u.ac.jp*

*Received August 31, 2005*

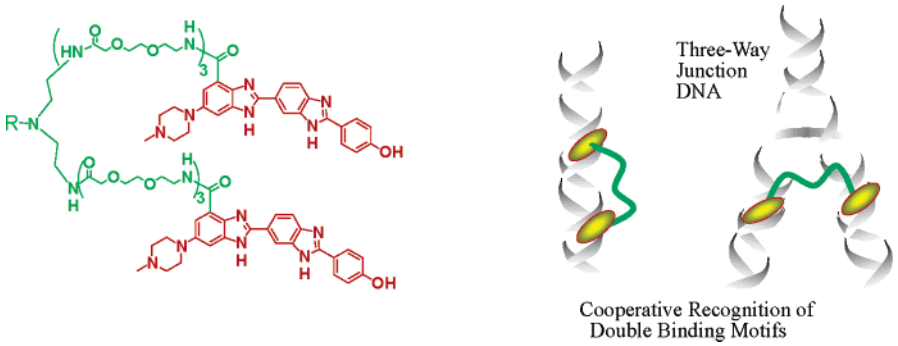


The aim of this study is to develop bidentate minor-groove binders that bind the double binding motifs cooperatively. The new bidentate ligands (**1**) have been designed by connecting two Hoechst 33258 units with a polyether linker for cooperative binding with two remote $A_3T_3$ sites of DNA. The linker is introduced to the benzimidazole ring so that it is located at the convex side of the Hoechst unit. DNA binding affinity of the ligands was evaluated by measuring surface plasmon resonance (SPR), circular dichroism, and fluorescence spectra. Interestingly, the bidentate ligands (**1**) did not show affinity to DNA**1** with a single $A_3T_3$ motif but showed selective affinity to DNA**2** with two $A_3T_3$ motifs. The Long Bis-H (**1L**) having a long polyether linker showed specific binding to DNA**2**(6) with two $A_3T_3$ motifs separated by six nonbinding base pairs. The Long Bis-H (**1L**) has also shown specific binding to the three-way junction DNA**4** with two $A_3T_3$ motifs. This study has demonstrated that DNA with double binding motifs can be selectively recognized by the newly designed bidentate ligands.

## Introduction

Molecules that bind duplex DNA sequence selectively have been of great interest because of potential applications in genomic studies as well as therapeutic purposes.[1−5] Small molecules are of special concern because they are easily accessible to chromosomal DNA.[6,7] Recent studies have shown that not only the sequences but also higher-ordered structures of DNA or RNA play significant roles in regulation of gene expression,[8−10] and therefore increasing attention has been paid to development of small molecular ligands for targeting such structures. Triplex-binding ligands are used in antigene approach for inhibition of transcription,[11−13] and telomerase activity is inhibited by quadruplex-binding ligands.[14−16] Quadruplex-binding ligands were also used to detect G-quartet structure in

* To whom correspondence should be addressed. Tel: 81-92-642-6615. Fax: 81-92-642-6876.

(1) A recent review: Giovannangéli, C.; Hélène, C. *Curr. Opin. Mol. Ther.* **2000**, *2*, 288−296.

(2) Pooga, M.; Land, T.; Bartfai, T.; Langel, U. *Biomol. Eng.* **2001**, *17*, 183−192.

(3) Baraldi, P. G.; Bovero, A.; Fruttarolo, F.; Preti, D.; Tabrizi, M. A.; Pavani, M. G.; Romagnoli, R. *Med. Res. Rev.* **2004**, *24*, 475−528.

(4) Reddy, B. S. P.; Sharma, S. K.; Lown, J. W. *Curr. Med. Chem.* **2001**, *8*, 475−508.

(5) Sasaki, S.; Taniguchi, Y.; Takahashi, R.; Senko, Y.; Kodama, K.; Nagatsugi, F.; Maeda, M. *J. Am. Chem. Soc.* **2004**, *126*, 516−528.

(6) Dervan, P. B.; Poulin-Kerstien, A. T.; Fechter, E. J.; Edelson, B. S. *Top. Curr. Chem.* **2005**, *253*, 1−31.

(7) Melander, C.; Burnett, R.; Gottesfeld, J. M. *J. Biotechnol.* **2004**, *112*, 195−220.

(8) Catasti, P.; Chen, X.; Mariappan, S. V. S.; Bradbury, E. M.; Gupta, G. *Genetica* **1999**, *106*, 15−36.

(9) Shlyakhtenko, L. S.; Hsieh, P.; Grigoriev, M.; Potaman, V. N.; Sinden, R. R.; Lyubchenko, Y. L. *J. Mol. Biol.* **2000**, *296*, 1169−1173.

(10) Pearson, C. E.; Zorbas, H.; Price, G. B.; Zannis-Hadjopoulos, M. *J. Cell. Biochem.* **1996**, *63*, 1−22.

10.1021/jo051836t CCC: $33.50 
Published on Web 11/25/2005

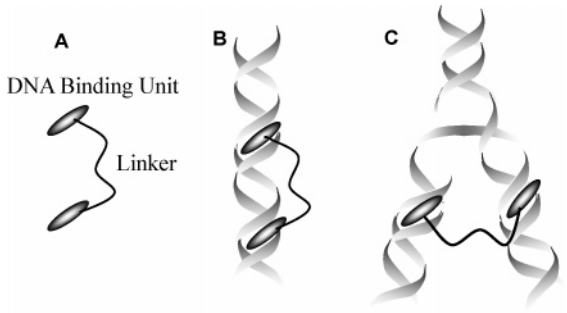


**FIGURE 1.** General concept for the molecular design of the bidentate ligand: (A) conceptual structure of the bidentate ligand; (B) cooperative binding to nearby binding sites in a canonical duplex DNA; (C) possible binding to distant sites in proximity of branched DNA.

cells.[17] The expanded minor-groove binder has been shown to form a complex with two remote binding sites at a distance of approximately 70 base pairs to each other in nucleosomal DNA.[18] RNA functions are inhibited specifically by RNA-binding ligands.[19−22] Inspired by these successful examples, we became interested in the development of small molecular ligands for branched DNA junctions that are involved in a variety of biological processes such as homologous recombination[23] or repair.[24] There are a number of binding proteins for branched DNA structures, but only a few studies have determined small molecular binders.[25−27] In this study, we have attempted to establish a new design concept of small molecular ligands for such higher-order DNA structure. Our approach relies on a general structure of branched DNA that brings each arm into proximity to the other and a bidentate ligand connecting two binder structures with an appropriate linker (Figure 1). If two binding domains of a bidentate ligand could interact with two remote regions of DNA cooperatively, such a bidentate ligand would show high affinity toward a specific DNA site where two distant binding motifs are located in close proximity to each other either in a canonical duplex (Figure 1B) or in junction DNA structures (Figure 1C). Here we wish to report in detail the molecular design of new bidentate ligands, their synthesis. and their selective binding to the DNA with nearby binding sites.

## Results

**Design of Bis-Hoechst Ligands.** Hoechst 33258, a representative minor-groove binder with high specificity to a sequence of $(A_3T_3)_2$,[28−30] was chosen as a basic unit to construct bidentate ligands (**1**). A polyethyleneoxy chain was used as a linker by expecting flexibility in conformation and low affinity with the phosphate backbone or base pairs. Introduction of the linker at the convex side of the curvature of the Hoechst skeletons would be advantageous in the point that the linker is stretched out to the groove exterior over the phosphate backbone to hold two minor groove binders within the complex with two DNA duplexes as shown in Figure 2.

**Synthesis of Bis-Hoechst Ligands.** The carboxy-substituted Hoechst derivatives were synthesized starting with 3,4-dinitrobenzoic acid (**2**) and 3-amino-5-chloro-2-nitrobenzoic acid (**5**) by modification of the reported method[31] (Scheme 1). The carboxylic acid of **2** was transformed to the Weinreb amide, and the nitro groups were reduced to the corresponding diamine (**3**). The diamino group was condensed with the *p*-hydroxybenzaldehyde, and the Weinreb amide was reduced to an aldehyde group to yield the benzimidazole intermediate (**4**). The *N*-methylpiperazine derivative (**6**) was obtained by esterification and following substitution of chloride of **5**.[32] The nitro group of **6** was reduced to the corresponding diamine, which was coupled with **4**, and then hydrolysis of the product gave the Hoechst intermediate (**7**).

Synthesis of the bis-Hoechst ligands (**1**) was carried out by solid-phase synthesis (Scheme 2). Fmoc-amino acids (**17** and **18**) were introduced to the resin, and the Fmoc protecting group was removed to give the amino-terminal resin **8** or **11**, respectively. Each resin was subjected to further coupling with **18** for elongation of the linker. Finally, the carboxy-substituted Hoechst intermediate **7** was applied to the resin, and the linker-bearing Hoechst ligands (**10**, **12**, and **13**) were cleaved from the resin with 10% TFA in $CH_2Cl_2$.

In the meantime, the anchor unit that is used to immobilize the bis-Hoechst ligand onto the SPR sensor chip was synthesized on the commercially available resin (**14**) with a diaminoether linker unit. The anchor of **14** was elongated with **18** for two cycles and then coupled with **19** to give the bis-amino terminal (**16**). The linker-containing Hoechst intermediates (**10**, **12**, and **13**) were coupled with **16**, and finally, the bis-Hoechst ligand was cleaved from the resin with TFA. The mono-Hoechst (**15**) as a reference compound having a long linker was also

(11) Bello-Roufai, M.; Roulon, T.; Escude, C. *Chem. Biol.* **2004**, *11*, 509−516.
(12) Keppler, M. D.; Neidle, S.; Fox, K. R. *Nucleic Acids Res.* **2001**, *29*, 1935−1942.
(13) Brown, P. M.; Drabble, A.; Fox, K. R. *Biochem. J.* **1996**, *314*, 427−432.
(14) Guittat, L.; De, C. A.; Rosu, F.; Gabelica, V.; De, P. E.; Delfourne, E.; Mergny, J. L. *Biochem. Biophys. Acta* **2005**, *1724*, 375−384.
(15) Rezler, E. M.; Seenisamy, J.; Bashyam, S.; Kim, M. Y.; White, E.; Wilson, W. D.; Hurley, L. H. *J. Am. Chem. Soc*. **2005**, *127*, 9439−9447.
(16) Damm, K.; Hemmann, U.; Garin-Chesa, P.; Hauel, N.; Kauffmann, I.; Priepke, H.; Niestroj, C.; Daiber, C.; Enenkel, B.; Guilliard, B.; Lauritsch, I.; Müller, E.; Pascolo, E.; Sauter, G.; Pantic, M.; Martens, U. M.; Wenz, C.; Lingner, J.; Kraut, N.; Rettig, W. J.; Schnapp, A. *EMBO J.* **2001**, *20*, 6958−6968.
(17) Siddiqui-Jain, A.; Grand, C. L.; Bearss, D. J.; Hurley, L. H. *Proc. Natl. Acad. Sci. U.S.A.* **2002**, *99*, 11593−11598.
(18) Edayathumangalam, R. S.; Weyermann, P.; Gottesfeld, J. M.; Dervan, P. B.; Luger, K. *Proc. Natl. Acad. Sci. U.S.A.* **2004**, *101*, 6864−6869.
(19) Tucker, B. J.; Breaker, R. R. *Curr. Opin. Struct. Biol.* **2005**, *15*, 342−348.
(20) Ryu, D. H.; Rando, R. R. *Bioorg. Med. Chem.* **2001**, *9*, 2601−2608.
(21) Dassonneville, L.; Hamy, F.; Colson, P.; Houssier, C.; Bailly, C. *Nucleic Acids Res.* **1997**, *25*, 4487−4492.
(22) Hwang, S.; Tamilarasu, N.; Ryan, K.; Huq, I.; Richter, S.; Still, W. C.; Rana, T. M. *Proc. Natl. Acad. Sci. U.S.A.* **1999**, *96*, 12997−13002.
(23) A recent review; Yamada, K.; Ariyoshi, M.; Morikawa, K. *Curr. Opin. Struct. Biol*. **2004**, *14*, 130−137.
(24) McGlynn, P.; Lloyd, R. G. *Trends Genet.* **2002**, *18*, 413−419.
(25) Carpenter, M. L.; Lowe, G.; Cook, P. R. *Nucleic Acids Res.* **1996**, *24*, 1594−1601.
(26) Guo, Q.; Lu, M.; Seeman, N. C.; Kallenbach, N. R. *Biochemistry* **1990**, *29*, 570−578.
(27) Kepple, K. V.; Boldt, J. L.; Segall, A. M. *Proc. Natl. Acad. Sci. U.S.A.* **2005**, *102*, 6867−6872.
(28) Spink, N.; Brown, D. G.; Skelly, J. V.; Neidle, S. *Nucleic Acids Res.* **1994**, *22*, 1607−1612.
(29) Vega, M. C.; Garcia-Saez, I.; Aymami, J.; Eritja, T.; Vander Marel, G. A.; Van Boom, J. H.; Rich, A.; Coll, M. *Eur. J. Biochem.* **1994**, *222*, 721−726.
(30) Haq, I.; Ladbury, J. E.; Chowdhry, B. Z.; Jenkins, T. C.; Chaires, J. B. *J. Mol. Biol.* **1997**, *271*, 244−257.
(31) Ji, Y.-H.; Bur, D.; Häsler, W.; Schmitt, V. R.; Dorn, A.; Bailly, C.; Waring, M. J.; Hoechstrasser, R.; Leupin, W. *Bioorg. Med. Chem.* **2001**, *9*, 2905−2919.
(32) Seko, S.; Miyake, K.; Kawamura, N. *J. Chem. Soc., Perkin Trans.* **1999**, *1*, 1437−1444.

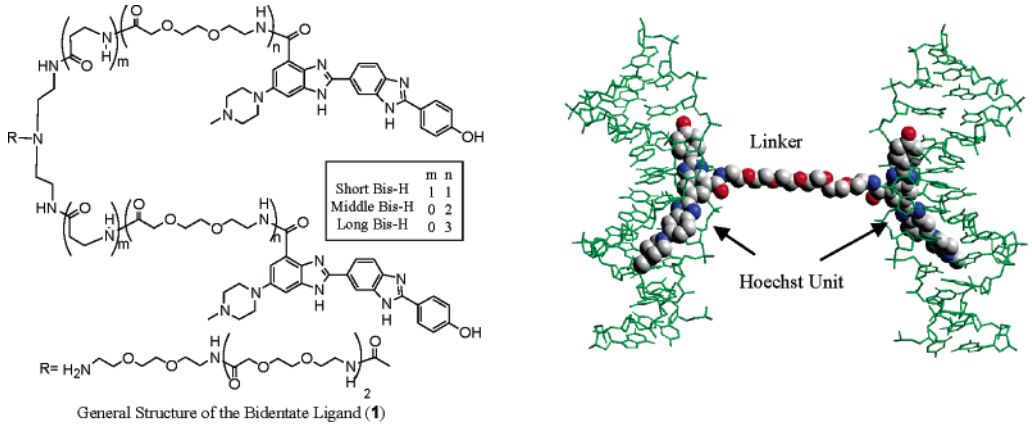


**FIGURE 2.** Expected complex between two duplexes and the bis-Hoechst ligand (**1**) connected with a polyethyleneoxy linker stretched out to the groove exterior.

**SCHEME 1**[a]

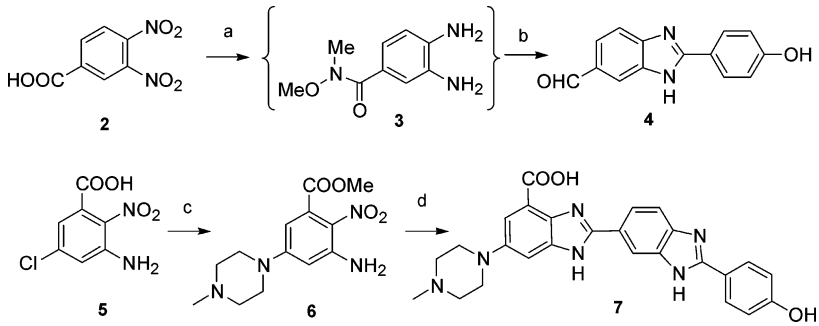

[a] (a) (1) $SOCl_2$, 80 °C, 3 h, (2) $CH_3ONHCH_3HCl$, pyridine, rt, 3.5 h, 65%; (3) $H_2$, 5% Pd−C, EtOH, rt; (b) (1) *p*-hydroxybenzaldehyde, $Na_2S_2O_5$, EtOH, $H_2O$, reflux, 6 h, 50%; (2) $LiAlH_4$, THF, −78 to 0 °C, 46 h, 84%; (c) (1) MeOH, $H_2SO_4$, reflux, 90 h, 74%, (2) *N*-methylpiperazine, $K_2CO_3$, 3.5 h, 52%; (d) (1) $H_2$, 5% Pd−C, EtOH, rt, 6.5 h, (2) **4**, $Na_2S_2O_5$, EtOH, $H_2O$, reflux, 20 h, 94%, (3) 10% aqueous NaOH, 70 °C, 30 min, 84%.

synthesized similarly. The bis-Hoechst ligands (**1**) are named according to the length of the linker: Short Bis-H (**1S**; *m*,*n* = 1,1), Middle Bis-H (**1M**; *m*,*n* = 0,2), and Long Bis-H (**1L**; *m*,*n* = 0,3). All products were purified by HPLC and their structures were confirmed by MS, NMR measurements.

**Evaluation of DNA Binding Properties. Surface Plasmon Resonance (SPR).** The Hoechst ligand containing the amino terminal anchor unit (**1**, **15**) was dissolved in acetate buffer (pH 4.5, 10 $\mu$M) and immobilized on a sensor chip CM5 (carboxymethylated dextran surface) using amine coupling kit in HBS-N running buffer (0.01 M HEPES, 0.15 M NaCl, pH 7.4) at 25 °C. The amounts of the immobilized ligand were monitored and quantified by an increase of the SPR signal to be within the range from $6.2 \times 10^{-10}$ to $1.7 \times 10^{-9}$ fmol/nm$^2$, implying that one ligand molecule is immobilized in every 3−10 nm$^2$. DNA samples (DNA**1** and **2**, Figure 3) were annealed prior to the binding analysis by heating to 80 °C for 3 min and slowly cooled to room temperature. SPR measurements were performed in HBS-N running buffer at 25 °C. The reference response from the blank cell was subtracted from the response in the channel with the immobilized ligand to give a signal (RU, resonance units) that is directly proportional to the amount of the bound compound. SPR sensorgrams of the different DNA samples at the same concentration for binding to the immobilized ligand are compared in Figure 4. A set of sensorgrams at different concentrations of the DNA samples (**1** and **2**(3)) for the mono- and bis-Hoechst ligands (**15**, **1S**, **1M**, and **1L**) were obtained to calculate complex stability constants from Scatchard plots (Table 1). As can be seen in the Figure 4A obtained with the mono-Hoechst ligand **15**, both association and dissociation of DNA**1** with a single $A_3T_3$ site are rapid. The binding constant obtained here is much lower than that of the parent Hoechst 33258 measured by ITC ($2.7 \times 10^4$ vs $3.2 \times 10^8$ M$^{-1}$).[30] It was anticipated in a similar biding study by SPR that the small ligand immobilized in the sensor surface would not be effectively exposed on the surface but would be folded back into the matrix as the result of a small molecular size and its hydrophobic character.[33] Strong binding affinity of the mono-Hoechst **15** to DNA**1** in solution has been proved by CD titration experiments as described in the subsequent section, indicating that the decrease in binding affinity of the immobilized mono-Hoechst **15** is probably due to such interfering factors. Figure 4A also indicates that DNA**2** with two $A_3T_3$ sites binds to the mono-Hoechst **15** stronger than DNA**1** regardless of the distance between the two $A_3T_3$ sites. As one molecule of the immobilized ligand is estimated to exist in every 3−10 nm$^2$, the neighboring ligands on the sensor chip are thought to be close enough to bind simultaneously two $A_3T_3$ sites of DNA**2**. Such a 2:1 ligand-to-DNA complex has been also shown by CD titration experiments using the free ligand **15** and DNA**2**(6) in the subsequent section.

In striking contrast to the mono-Hoechst ligand **15**, binding affinity of the bis-Hoechst ligand (**1**) to DNA**1** decreased considerably (Figure 4B−D). Each bis-Hoechst ligand with a linker of different length shows different SPR sensitivity

(33) Nakatani, K.; Kobori, A.; Kumasawa, H.; Saito, I. *Bioorg. Med. Chem. Lett.* **2004**, *14*, 1105−1108.

**SCHEME 2. Solid-Phase Synthesis of Linker-Bearing Hoechst Ligands**[a]

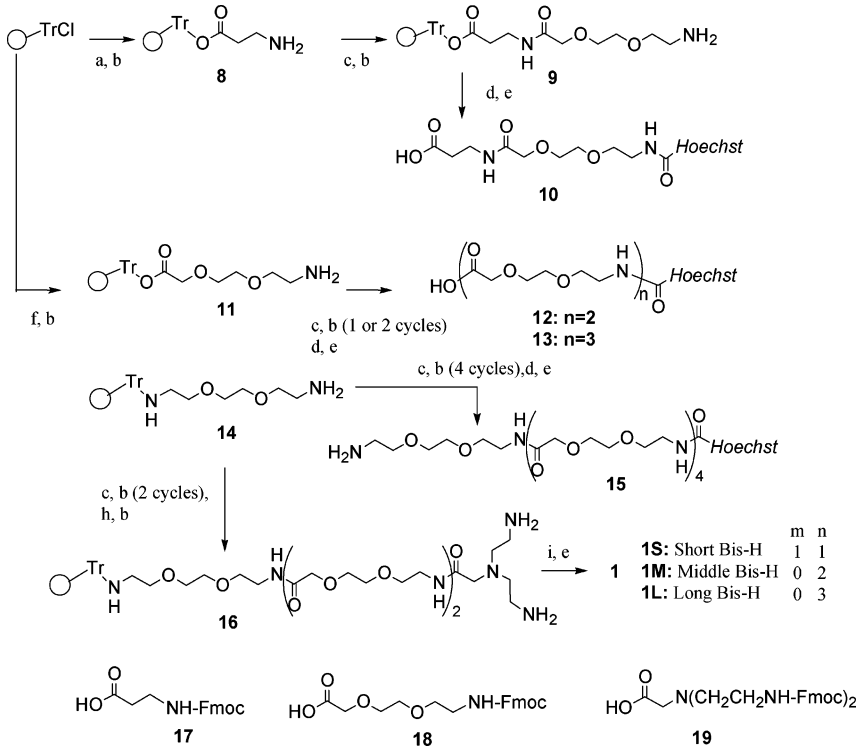


[a] (a) Fmoc-$\beta$-alanine (**17**), DIPEA, $CH_2Cl_2$; (b) 20% piperidine, DMF; (c) **18**, HBT, HBTU, DIPEA, NMP, DMF; (d) **7**, BOP, HBT, DMF, NMP; (e) 10% TFA in $CH_2Cl_2$; (f) **18**, DIPEA, $CH_2Cl_2$; (g) **12**, HBT, HBTU, DIPEA, NMP, DMF; (h) **19**, HBT, HBTU, DIPEA, NMP, DMF; (i) **10**, **12,** or **13**, HBT, HBTU, DIPEA, NMP, DMF.

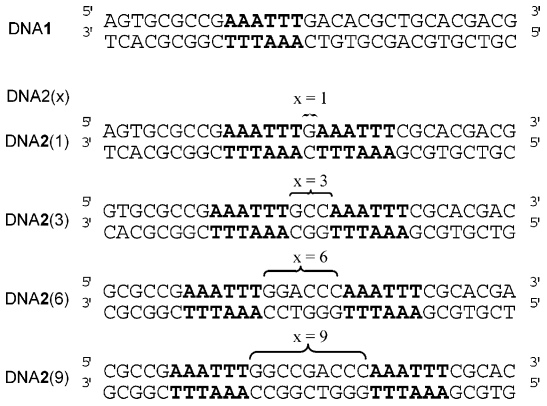


**FIGURE 3.** Sequences of the duplexes used in this study. DNA**1** contains a single $A_3T_3$ region, and DNA**2**(*x*) have two $A_3T_3$ regions separated by *x* number of nonbinding base pairs.

according to the distance between the two $A_3T_3$ sites in the order of DNA**2**(3) > DNA**2**(1), (6) > DNA**2**(9) ≫ DNA**1**. Despite differences in SPR sensitivity, calculated binding constants were not very much different (Table 1). SPR binding experiments have clearly demonstrated that the bis-Hoechst ligands selectively bind the DNA substrates with two $A_3T_3$ sites compared to the DNA substrate with a single $A_3T_3$ site.

As discussed in the analysis of the SPR sensorgrams obtained with the mono-Hoechst ligand **15**, sensorgrams with bis-Hoechst ligands may contain effects by the nearby ligands immobilized on the sensor chip. Decreased binding affinity of the mono-Hoechst ligand **15** has also suggested that binding of the Hoechst unit might be inhibited by its interaction with the matrix on the sensor surface. Thus, it turned out that measurement of binding affinity on the SPR sensor chip did not produce precise binding parameters in this study. We next examined DNA binding in solution to determine specificity of the bis-Hoechst ligand. The Long Bis-H (**1L**; *m*,*n* = 0,3) was used for further investigation in solution as a representative bis-Hoechst ligand, since it discriminates the DNA substrates most effectively in the SPR experiments.

**Fluorescent Spectra Measurements.** The fluorescent spectra of mono-Hoechst ligand **15** showed high intensity even in the absence of the DNA substrates (Figure 5A), and the DNA substrates (**1** and **2**) were not discriminated. As shown in Figure 5B, fluorescent intensity of Long Bis-H (**1**; *m*,*n* = 0,3) is increased to a larger extent in the presence of DNA with two $A_3T_3$ sites (DNA**2**) than in the presence of DNA**1** with a single $A_3T_3$ site, again demonstrating the selectivity of Long Bis-H (**1L**; *m*,*n* = 0,3) to the DNA substrates with two $A_3T_3$ sites. Attempts to determine binding constants by these fluorescent spectra changes were unsuccessful, because the spectral intensity and maximum wavelength gradually changed during titration.

**Circular Dichroism Spectra Measurements.** It has been reported that the binding of Hoechst 33258 to DNA is accompanied by CD spectral changes between 200 and 300 nm (the DNA region) and between 300 and 400 nm (a binding-induced CD band of Hoechst 33258).[34] CD titration profiles were measured by adding aliquots of the Hoechst ligand to a DNA solution. The ligand concentrations were in the range of 0−20 $\mu$M. Figure 6 summarizes the results with Long Bis-H (**1L**; *m*,*n* = 0,3), mono-Hoechst **15**, and DNA**1** or DNA**2**(6). The CD spectrum of DNA**2**(6) was changed by the addition of Long Bis-H (**1L**) with isoelliptic points at 257 and 284 nm (Figure 6A), suggesting a single binding mode in relation to

(34) Han, F.; Taulier N.; Chalikian, T. V. *Biochemistry* **2005**, *44*, 9785−9794.

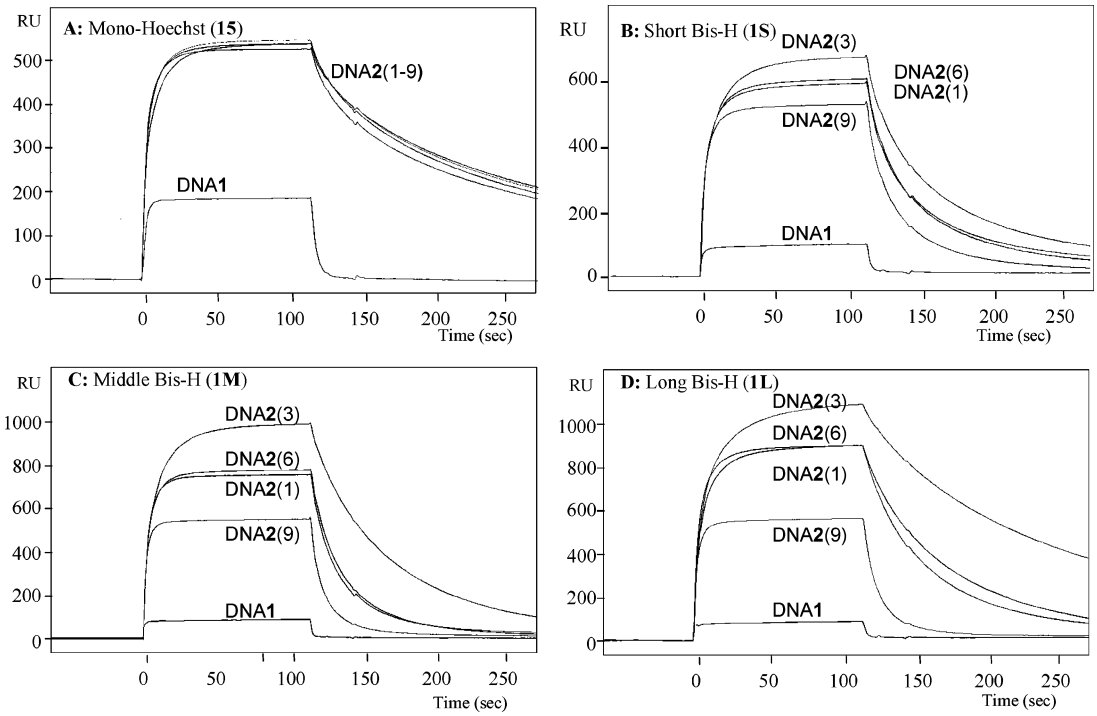


**FIGURE 4.** SPR measurement was performed with use of the sensor chip immobolizing Hoechst ligand (**1** or **15**). DNA duplexes (**1**, **2**, 10 $\mu$M) were injected during 0−120 s in HBS-N buffer, at pH 7.4, 25 °C.

**TABLE 1. Complex Stability Constants Obtained from SPR Measurements**[a]

| ligand | DNA | $K_a$ ($M^{-1}$) |
|---|---|---|
| **15** | DNA**1**[b] | $2.7 \times 10^4$ |
| | DNA**2**(3)[c] | $2.6 \times 10^6$ |
| Short Bis-H | DNA**2**(1) | $3.5 \times 10^5$ |
| | DNA**2**(3) | $3.4 \times 10^5$ |
| | DNA**2**(6) | $3.2 \times 10^5$ |
| | DNA**2**(9) | $2.8 \times 10^5$ |
| Middle Bis-H | DNA**2**(1) | $3.2 \times 10^5$ |
| | DNA**2**(3) | $4.3 \times 10^5$ |
| | DNA**2**(6) | $3.2 \times 10^5$ |
| | DNA**2**(9) | $2.4 \times 10^5$ |
| Long Bis-H | DNA**2**(1) | $5.0 \times 105$ |
| | DNA**2**(3) | $3.2 \times 10^5$ |
| | DNA**2**(6) | $4.5 \times 10^5$ |
| | DNA**2**(9) | $2.4 \times 10^5$ |

[a] Complex stability constants were obtained from Scatchard plots except for the data with ligand **15**. The binding parameters with the ligand **15** were calculated by a built-in program using the following binding modes: (*b*) Langmuir 1:1 binding, (*c*) bivalent 2:1 ligand-to-DNA binding.

the conformation of DNA**2**(6). Figure 6B represents a titration curve obtained by plotting the changes of ellipticity at 275 nm, and clearly indicates that complexation between Long Bis-H (**1**; *m*,*n* = 0,3) and DNA**2**(6) takes place in a 1:1 ratio with high affinity of $K_s = 6.6 \times 10^7$ $M^{-1}$. Long Bis-H (**1L**; *m*,*n* = 0,3) induced too small CD changes with DNA**1** to calculate the binding affinity. The results with SPR, UV, and CD have clearly indicated that Long Bis-H (**1L**; *m*,*n* = 0,3) has selective affinity to DNA**2** and not to DNA**1**. In similar CD titration experiments, the titration curve obtained with use of mono-Hoechst ligand **15** and DNA**1** represents 1:1 ligand-to-DNA**1** binding (Figure 6C), and that obtained with **15** and DNA**2**(6) shows 2:1 ligand-to-DNA complexation (Figure 6D). Binding constants of these complexes are similar to the reported value of the parent Hoechst 33258 ($K_s = 3.2 \times 10^8$, $M^{-1}$),[30] indicating that the Hoechst unit of **15** bind the two $A_3T_3$ sites of DNA**2** independently. The binding constants of Long Bis-H with other DNA substrates are summarized in Table 2 and have clearly demonstrated that Long Bis-H (**1L**; *m*,*n* = 0,3) exhibits selective binding to DNA**2**(6) with two $A_3T_3$ sites separated by six nonbinding base pairs.

**Application of the Long Bis-Hoechst Ligand to Recognition of the Junction DNA.** The results described above have suggested that two Hoechst units of the Long Bis-H (**1L**; *m*,*n* = 0,3) can bind two $A_3T_3$ sites simultaneously and discriminate the distance between them. Therefore, we further examined binding properties of Long Bis-H (**1L**, *m*,*n* = 0,3) toward junction DNA structures as a model of highly ordered DNA. The junction sequences were designed according to ref 35. The junction DNA**3** and **4** were formed by mixing the three strands A, B, and C (Figure 7), and its formation was analyzed by gel electrophoresis with nondenatured polyacrylamide gel, followed by isolation of the corresponding band and MALDI-TOF MS measurements of the contained three strands. Junction DNA**4**(*x*,*y*) having a single or two $A_3T_3$ sites was also synthesized using the corresponding strands (A, B, and C). The positions of $A_3T_3$ sites in the junction DNA**4**(*x*,*y*) are named after the number of bases *x* and *y* from the junction point, as shown in Figure 7.

The binding of Long Bis-H to the junction DNA **3** and **4** was analyzed by SPR (Figure 8A). Although DNA**3** contains no $A_3T_3$ site, weak binding with slow association and dissociation rates was observed. A junction site may provide a weak binding pocket to a Hoechst unit such as reported in binding with the CC bulge site of RNA.[36] Such additional binding may result in relatively strong binding of Long Bis-H (**1L**; *m*,*n* = 0,3) with the junction DNA**4**(14, null) with a single $A_3T_3$ site. This binding property shows a contrast to the nonbinding ability observed with a straight duplex DNA**1** (Figure 4D).

(35) Assenberg, R.; Weston, A.; Cardy, D. L.; Fox, K. R. *Nucleic Acids Res.* **2002**, *30*, 5142−5150.
(36) Cho, J.; Rando, R. R. *Nucleic Acids Res.* **2000**, *28*, 2158−2168.

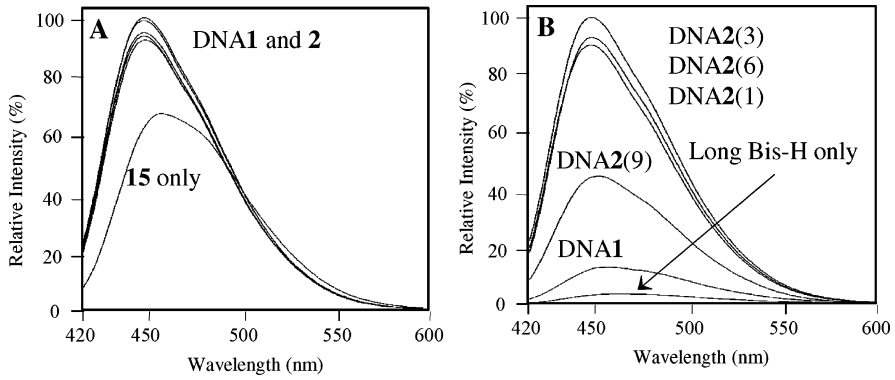


**FIGURE 5.** Fluorescence spectra of mono-Hoechst (**15**) and Long Bis-H(**1**) changed in the absence and presence of DNA. Measurements were performed using 100 nM each of the ligand and the DNA in the buffer at pH 7.4 with excitation wavelength at 370 nm.

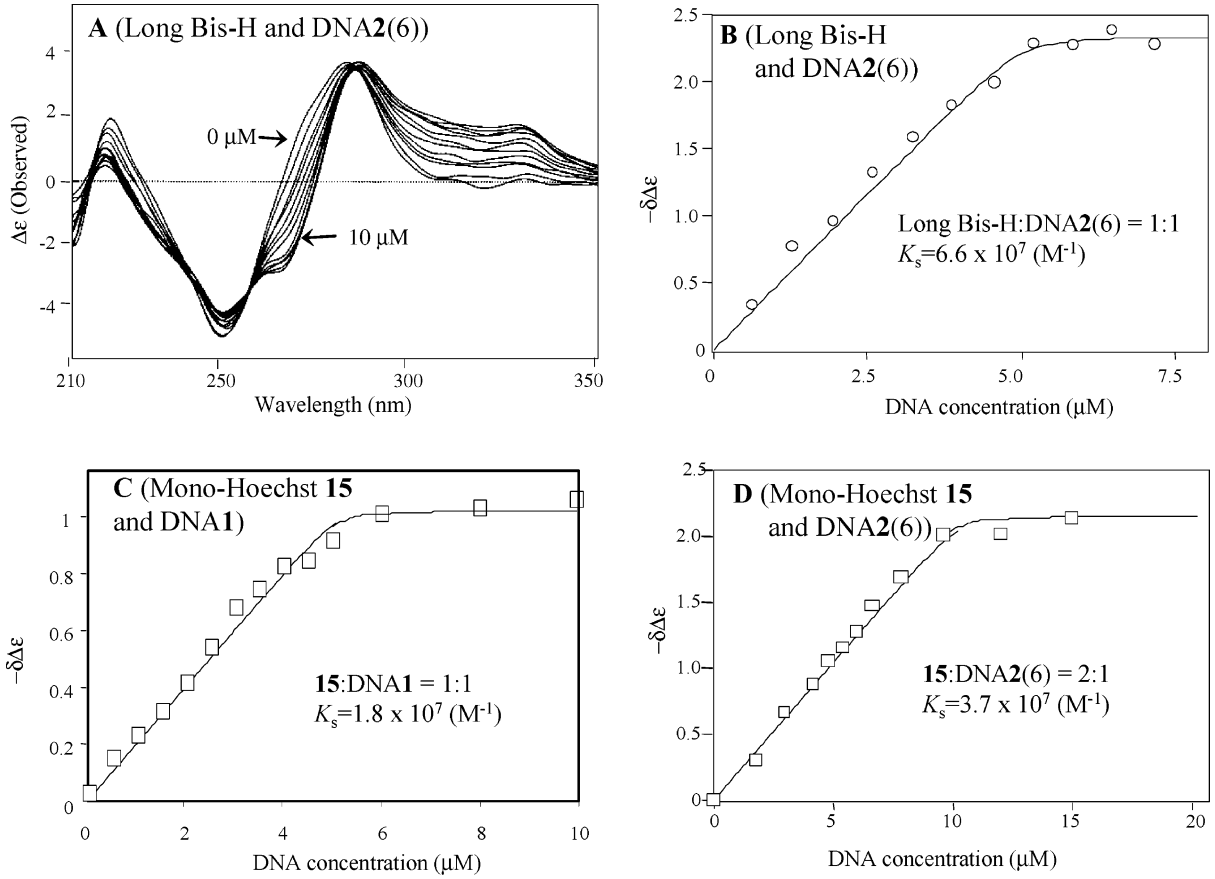


**FIGURE 6.** CD spectra in the presence and absence of the Hoechst ligand: (A) CD spectra change of DNA**2**(6) in the presence of Long Bis-H; (B−D) changes of ellipticity at 275 nm are plotted against the concentration of the ligand. CD spectra were measured using 5 $\mu$M DNA and the ligand ranging from 0 to 20 $\mu$M.

**TABLE 2. Binding Constants of the Long Bis-H (1L)**

| | $K_s$ ($M^{-1}$)[a] |
|---|---|
| DNA**1** | *b* |
| DNA**2**(1) | $1.2 \times 10^5$ |
| DNA**2**(3) | $3.0 \times 10^5$ |
| DNA**2**(6) | $6.6 \times 10^7$ |
| DNA**2**(9) | $2.2 \times 10^6$ |

[a] Calculated from the titration curve, such as shown in Figure 6C. [b] Binding is too weak to obtain binding constant under the same conditions.

The junction DNA**4** having two $A_3T_3$ sites exhibits higher affinity compared to DNA**4** with a single or no $A_3T_3$ binding motif. Long Bis-H (**1L**) binds the junction DNA**4**(14,10) having two $A_3T_3$ sites showed higher SPR sensitivity than to the junction DNA**4**(14,null) with a single $A_3T_3$ site. However, the position of $A_3T_3$ sites in the junction structure is not clearly discriminated in the sensorgrams. In the CD titration experiments, isoelliptic points are observed at 255 and 287 nm, suggesting a single binding mode in relation to the junction DNA structure. Small CD changes indicate that complexation induces a little conformational change compared to the binding with the linear DNA**3** (Figures 6A vs 8B). From a titration curve obtained by plotting the changes of ellipticity at 275 nm, the binding parameter of 1:1 complexation with the binding constant $K_s = 2.1 \times 10^5$ ($M^{-1}$) was calculated. The two $A_3T_3$ sites of DNA**4**(14,10) are apart in the sequence (24 base pairs), but

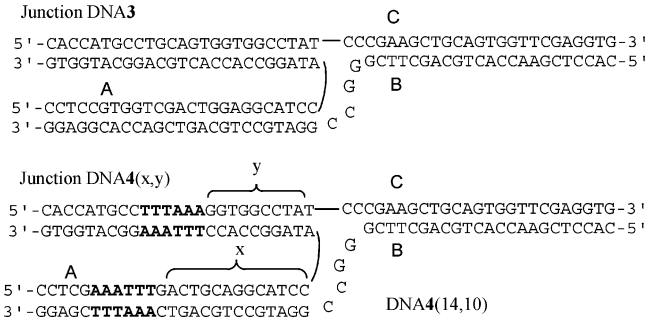


**FIGURE 7.** General structures of the junction DNA**3** and **4**. Junction DNA**3** (control) represents the basic junction sequence having no $A_3T_3$ site. The numbers *x* and *y* in DNA**4**(*x*,*y*) represent the number of base pairs from the junction point as shown in an example of DNA**4**(14,-10). DNA**4**(14, null) has only a single $A_3T_3$ site at the position $x = 14$.

should be close together in space in the junction conformation to be bound by two Hoechst unit of Long Bis-H (**1L**).

## Discussion

**Selectivity to the DNA Duplexes with Two $A_3T_3$ Binding Motifs.** The CD titration experiments have clearly shown that the Long Bis-H (**1L**) is highly selective to the DNA duplexes with two $A_3T_3$ binding motifs. This property is interesting, because the mono-Hoechst attaching a polyether linker retains strong binding affinity to a single $A_3T_3$ site (Figures 4A, 6C). The MD and MM calculations of the free Long Bis-H (**1L**) have suggested a self-aggregated conformation, in which Hoechst units are stacked to each other and the polyether linker is coiled around itself (Figure 9). In the three binding studies by SPR, fluorescence, and CD titration, the Bis-Hoechst **1** did not show affinity to DNA**1** with a single $A_3T_3$ site. From these results, the possibility of binding of a stacked Hoechst dimer with a single $A_3T_3$ site is excluded. Instead, such a stacked conformation of the Long Bis-H (**1L**) may become disadvantageous for binding with a $A_3T_3$ site. Thus, it may be reasonably assumed that two Hoechst units of the unwound Bis-Hoechst **1** bind with two $A_3T_3$ sites of the DNA**2** in such a way as illustrated in Figure 10. The distances between the two Hoechst units depend on the extent of unwinding of the linker of the Long Bis-H (**1L**). The linker may be partially coiled in the complex with DNA**2** (Figure 10A), and it may be fully extended in the complex with the junction DNA**4** (Figure 10B). A search

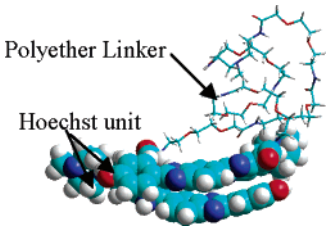


**FIGURE 9.** Molecular modeling of the Long Bis-H. MD and MM were performed with the AMBER force field.

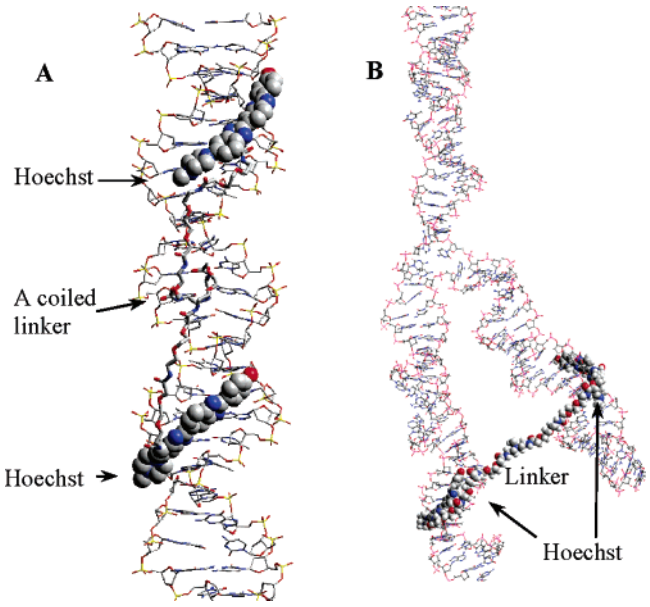


**FIGURE 10.** Illustrations of the simulated complexes of the Long Bis-H with the duplex DNA**2**(6) (A) and that with the junction DNA **4**(14,10) (B). MD and MM were performed with AMBER 94 force field.

for appropriate linkers will be a crucial step to determine more specific ligands toward each DNA structure in further studies.

## Conclusion

In conclusion, this study has revealed that new ligands connecting two Hoechst units through a polyether linker show specific affinity to DNA having two $A_3T_3$ motifs and that the distance between the two $A_3T_3$ motifs can be recognized depend-

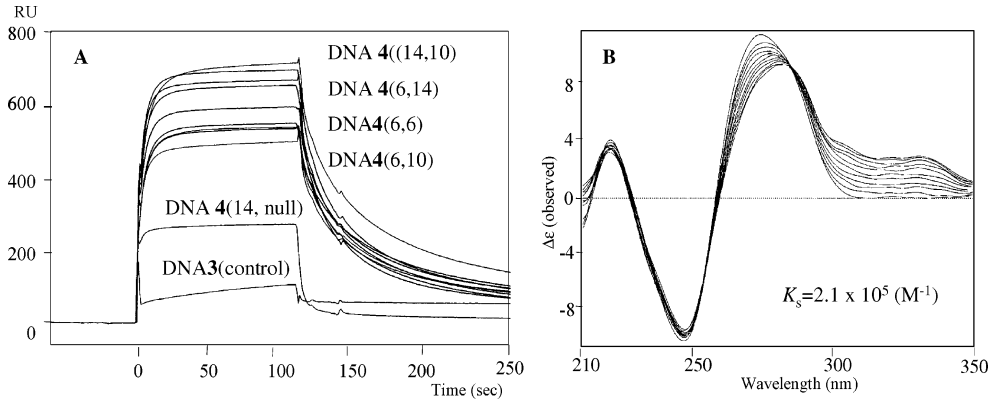


**FIGURE 8.** SPR Sensorgrams obtained with immobilized Long Bis-H (**1L**) (A) and CD spectra change of DNA**4**(14,10) in the presence of Long Bis-H (**1L**) (B). SPR measurements were performed using 10 $\mu$M DNA in the HBS-N buffer at pH 7.4 at 25 °C, CD spectra were measured using 5 $\mu$M DNA and the ligand ranging from 0 to 20 $\mu$M.

ing on the length of the linker. As an interesting application of the new ligand, binding to the junction DNA has been achieved. As a first approach for recognition of highly ordered DNA structure, this study has represented a reliable molecular basis to design junction-specific DNA-binding molecules.

## Experimental Section

***N*-Methoxy-*N*-methyl-3,4-diaminobenzamide (3).** Under argon, a mixture of thionyl chloride (25 mL) and 3,4-dinitrobenzoic acid (**2**) (10 g, 47.1 mmol) was heated at 80 °C. After 3 h, the reaction mixture was concentrated under reduced pressure. The residue was subjected to toluene azeotrope to give the corresponding acid chloride as a brown oil. Under argon, to a solution of the above acid chloride in $CH_2Cl_2$ (50 mL) was added pyridine (6.9 mL, 85.3 mmol) and *N*,*O*-dimethylhydroxylamine hydrochloride (5.72 g, 58.6 mmol) at 0 °C, and then the mixture was stirred at room temperature. After 3.5 h, the reaction mixture was diluted with $CH_2Cl_2$ and washed with $H_2O$ and brine. The organic layer was dried over $Na_2SO_4$ and concentrated under reduced pressure. The residue was recrystallized from diethyl ether to give *N*-methoxy-*N*-methyl-3,4-dinitrobenzamide (7.79 g, 65%) as a pale yellow solid: mp 95−96 °C; IR (powder) $cm^{-1}$ 1639, 1535, 1360; $^1H$ NMR (270 MHz, $CDCl_3$) $\delta$ 8.30 (d, $J$ = 1.6 Hz, 1H), 8.11 (dd, $J$ = 1.6, 8.3, 1H), 7.96 (d, $J$ = 8.3 Hz, 1H), 3.59 (s, 3H), 3.43 (s, 3H); $^{13}C$ NMR (100 MHz, $CDCl_3$) $\delta$ 164.7, 143.4, 142.2, 139.0, 133.5, 125.4, 124.8, 61.7, 33.0.

A solution of the above product (6.37 g, 25 mmol) in EtOH (200 mL) was hydrogenated over 5% Pd/C (4 g) for 4 h at room temperature. The reaction mixture was used for the next reaction without purification.

**2-(4-Hydroxyphenyl)-3*H*-benzoimidazole-5-carbaldehyde (4).** A mixture of the above mixture, a solution of sodium pyrosulfite (4.54 g, 23.9 mmol) in $H_2O$ (6 mL), and *p*-hydroxybenzaldehyde (3.36 g, 27.5 mmol) was heated at reflux. After 6 h, the reaction mixture was cooled to room temperature and filtered through a bed of Celite to remove the catalyst. The filtrate was concentrated under reduced pressure. The residue was washed with MeOH to give 2-(4-hydroxyphenyl)-3*H*-benzoimidazole-5-carboxylic acid *N*-methoxy-*N*-methylamide (3.69 g, 50%) as a beige powder: mp 281−282 °C; IR (powder) $cm^{-1}$ 3245, 1613, 1576, 1380; $^1H$ NMR (400 MHz, MeOH-$d_4$) $\delta$ 10.00 (s, 0.5H), 9.99 (s, 0.5H), 8.00 (d, $J$ = 8.6 Hz, 2H), 7.86 (s, 0.5H), 7.75 (s, 0.5H), 7.62−7.42 (m, 3H), 6.91 (d, $J$ = 8.9 Hz, 2H), 3.61 (s, 3H), 3.39 (s, 3H); $^{13}C$ NMR (100 MHz, $CDCl_3$) $\delta$ 169.8, 159.5, 153.7, 128.4, 127.4, 122.4, 120.7, 118.4, 117.6, 115.8, 110.5, 60.5, 33.7; HRMS (APCI) *m*/*z* calcd for $C_{16}H_{16}N_3O_3$ ($[M + H]^+$) 298.1186, found 298.1179.

Under argon, to a suspension of the above product (972 mg, 3.27 mmol) in THF/diethyl ether (3/1, 120 mL) was added $LiAlH_4$ (380 mg, 13.3 mmol) at −40 °C, and then the reaction mixture was stirred at 4 °C. After 46 h, the mixture was poured into saturated $NH_4Cl$/ice (1/1) and stirred for 10 min. The solution was extracted with EtOAc, and the organic layer was dried over $Na_2SO_4$ and concentrated under reduced pressure. The residue was triturated with EtOAc/diethyl ether (1/1) to afford **4** (654 mg, 84%) as a pale yellow powder: mp >300 °C; IR (powder) $cm^{-1}$ 3300−3100, 1611, 1286; $^1H$ NMR (500 MHz, DMSO-$d_6$) $\delta$ 10.02 (s, 1H), 8.07−8.06 (m, 1H), 8.03 (d, $J$ = 8.9 Hz, 2H), 7.73−7.68 (m, 3H), 6.93 (d, $J$ = 8.7 Hz, 2H); $^{13}C$ NMR (100 MHz, DMSO-$d_6$) $\delta$ 192.5, 159.9, 159.2, 156.2, 152.0, 131.3, 130.9, 128.7, 128.2, 123.4, 123.0, 121.2, 120.4, 115.9, 115.7, 114.9; HRMS (APCI) *m*/*z* calcd for $C_{14}H_{11}N_2O_2$ ($[M + H]^+$) 239.0815, found 239.0809.

**3-Amino-5-chloro-2-nitrobenzoic Acid (5).** Under argon, to a solution of potassium *tert*-butoxide (94 g, 838 mmol) and copper(II) acetate monohydrate (2.2 g, 12.1 mmol) in DMF (400 mL) was added a solution of *O*-methylhydroxylamine hydrochloride (20 g, 239 mmol) and 3-chloro-6-nitrobenzoic acid (25 g, 124 mmol) in DMF (400 mL) at 0 °C. After 3 h, the reaction mixture was quenched by addition of $H_2O$ and acidified with 10% HCl. The mixture was extracted with EtOAc. The organic layer was dried over $Na_2SO_4$ and concentrated under reduced pressure. The residue was dissolved in EtOAc and extracted with 10% NaOH. The aqueous layer was acidified with concentrated HCl and extracted with EtOAc. The organic layer was dried over $Na_2SO_4$ and concentrated under reduced pressure. The crude product was recrystallized from hexane/EtOAc to give **5** (10.3 g, 32%) as an orange solid: mp 183−184 °C; IR (powder) $cm^{-1}$ 3489, 3377, 1707, 1609, 1572;$^1H$ NMR (400 MHz, DMSO-$d_6$) $\delta$ 7.12 (d, $J$ = 2.3 Hz, 1H), 7.06 (s, 2H), 6.75 (d, $J$ = 2.1 Hz, 1H); $^{13}C$ NMR (100 MHz, $CDCl_3$) $\delta$ 166.2, 145.2, 137.8, 133.1, 129.2, 118.9, 115.3.

**3-Amino-5-(4-methylpiperazin-1-yl)-2-nitrobenzoic Acid Methyl Ester (6).** Under argon, to a solution of **5** (6.75 g, 31.2 mmol) in absolute MeOH (200 mL) was added $H_2SO_4$ (2 mL), and the mixture was heated at reflux. After 90 h, the reaction mixture was neutralized with powdered $Na_2CO_3$. The mixture was diluted with $H_2O$ and extracted with EtOAc. The organic layer was dried over $Na_2SO_4$ and concentrated under reduced pressure. Column chromatography (silica gel, hexane/EtOAc, 2/1 to 1/1) afforded 3-amino-5-chloro-2-nitrobenzoic acid methyl ester (5.33 g, 74%) as a red solid. The aqueous layer was acidified with 10% HCl and extracted with EtOAc. The organic layer was dried over $Na_2SO_4$ and concentrated under reduced pressure to recover **5** (1.19 g, 16%) as a brown solid: mp 106−107 °C; IR (powder) $cm^{-1}$ 3464, 3352, 1717, 1570, 1290; $^1H$ NMR (500 MHz, DMSO-$d_6$) $\delta$ 6.90 (d, $J$ = 2.3 Hz, 1H), 6.80 (d, $J$ = 2.3 Hz, 1H), 5.86 (br, 2H), 3.90 (s, 3H); $^{13}C$ NMR (100 MHz, $CDCl_3$) $\delta$ 166.3, 144.4, 140.3, 132.8, 129.6, 119.4, 118.1, 53.3; HRMS (ESI) *m*/*z* calcd for $C_8H_7ClN_2O_4Na$ ($[M + Na]^+$) 252.9987, found 252.9983.

Under argon, to a solution of 3-amino-5-chloro-2-nitrobenzoic acid methyl ester (100 mg, 0.43 mmol) in DMF (2 mL) was added *N*-methylpiperazine (273 $\mu$L, 2.46 mmol) and potassium carbonate (341 mg, 2.47 mmol), and the solution was heated at 105 °C. After 3.5 h, the reaction mixture was filtered and concentrated under reduced pressure. Column chromatography (silica gel, $CHCl_3$/MeOH, 8/1 to 6/1) afforded **6** (66 mg, 52%) as a red solid: mp 160−161 °C; IR (powder) $cm^{-1}$ 3406, 3263, 1728, 1605, 1572; $^1H$ NMR (270 MHz, $CDCl_3$) $\delta$ 6.33 (d, $J$ = 2.6 Hz, 1H), 6.13 (br, 2H), 5.97 (d, $J$ = 2.6 Hz, 1H), 3.89 (s, 3H), 3.38 (t, $J$ = 5.1 Hz, 4H), 2.52 (t, $J$ = 5.1 Hz, 4H), 2.35 (s, 3H); $^{13}C$ NMR (100 MHz, $CDCl_3$) $\delta$ 168.6, 153.8, 147.0, 124.3, 110.0, 106.5, 99.2, 54.4, 53.0, 46.7, 46.0; HRMS (ESI) *m*/*z* calcd for $C_{13}H_{19}N_4O_4$ ($[M + H]^+$) 295.1401, found 295.1448.

**2′-(4-Hydroxy-phenyl)-6-(4-methyl-piperazin-1-yl)-1*H*,3′*H*-[2,5′]bibenzoimidazolyl-4-carboxylic Acid (7).** A solution of **6** (500 mg, 1.07 mmol) in EtOH (25 mL) was hydrogenated over 5% Pd/C (500 mg) at room temperature. After 6.5 h, the reaction mixture was filtered through a bed of Celite to remove the catalyst and concentrated under reduced pressure to afford the corresponding diamine. To a solution of the above product in EtOH (25 mL) was added a solution of sodium pyrosulfite (168 mg, 0.88 mmol) in $H_2O$ (0.9 mL) and **4** (607 mg, 2.55 mmol), and then the reaction mixture was heated at reflux. After 20 h, the reaction mixture was concentrated under reduced pressure. Column chromatography (silica gel, diethyl ether/MeOH, 3/1 to 3/2) afforded the methyl ester of **7** (768 mg, 94%) as a yellow solid: mp 269−270 °C; IR (powder) $cm^{-1}$ 3500−2800, 1612, 1445; $^1H$ NMR (400 MHz, MeOH-$d_4$) $\delta$ 8.28 (s, 1H), 7.98 (d, $J$ = 8.4 Hz, 1H), 7.96 (d, $J$ = 8.8 Hz, 2H), 7.67 (d, $J$ = 8.4 Hz, 1H), 7.62 (d, $J$ = 2.3 Hz, 1H), 7.46 (d, $J$ = 2.1 Hz, 1H), 6.93 (d, $J$ = 8.8 Hz, 2H), 4.04 (s, 3H), 3.24 (t, $J$ = 5.0 Hz, 4H), 2.67 (t, $J$ = 4.9 Hz, 4H), 2.37 (s, 3H); $^{13}C$ NMR (125 MHz, DMSO-$d_6$) $\delta$ 165.8, 159.6, 154.5, 153.4, 145.3, 128.4, 123.3, 121.8, 120.5, 115.8, 114.7, 52.6, 52.2, 47.3, 42.2; HRMS (ESI) *m*/*z* calcd for $C_{27}H_{27}N_6O_3$ ($[M + H]^+$) 483.2139, found 483.2103.

A solution of the above methyl ester of **7** (1 g, 2.07 mmol) in 1 M NaOH (33 mL) was heated at 70 °C. After 30 min, the reaction

mixture was neutralized by 10% HCl and the resulting precipitate was filtered. The obtained solid was dried under reduced pressure over $P_2O_5$ to afford **7** (819 mg, 84%) as a yellow solid. Analytical sample was obtained by reverse-phase HPLC (Nacalai Tesque COSMOSIL 5C18-AR-300 20 mm × 250 mm; eluents $H_2O$ (A) and $CH_3OH$ (B); gradient 0−20 min, 40−50% B in A + B; flow rate 10 mL/min; detection 254 nm): mp 295−296 °C; IR (powder) $cm^{-1}$ 3500−2800, 1531, 1443; $^1H$ NMR (400 MHz, MeOH-$d_4$) $\delta$ 8.30 (s, 1H), 8.01−7.97 (m, 3H), 7.69 (d, $J$ = 8.4 Hz, 1H), 7.65 (d, $J$ = 2.1 Hz, 1H), 7.31 (d, $J$ = 2.1 Hz, 1H), 6.94 (d, $J$ = 8.6 Hz, 2H), 3.26 (t, $J$ = 4.7 Hz, 4H), 2.69 (t, $J$ = 4.8 Hz, 4H), 2.38 (s, 3H); $^{13}C$ NMR (125 MHz, DMSO-$d_6$/$D_2O$, 9/1) $\delta$ 166.5, 163.0, 151.9, 149.5, 148.4, 135.9, 135.6, 132.6, 130.7, 126.4, 125.7, 120.2, 118.5, 117.8, 117.5, 115.5, 113.6, 113.3, 107.7, 105.4, 53.6, 47.1, 43.7; HRMS (ESI) *m/z* calcd for $C_{26}H_{25}N_6O_3$ 469.1983 ([M + H]$^+$), found 469.1962.

**Bis[2-(9*H*-fluoren-9-ylmethoxycarbonylamino)ethyl]-aminoacetic Acid (19).** To a solution of $FmocNHCH_2CHO$[37] (1 g, 3.56 mmol) in MeOH (17 mL) and acetic acid (3 mL) were added glycine (107 mg, 1.43 mmol) and sodium cyanoborohydride (224 mg, 3.56 mmol) at room temperature. After 7 h, to the reaction mixture was added diethyl ether (30 mL), and resulting precipitate was filtered. The obtained solid was dissolved in 10% NaOH, and the solution was acidified at pH 2 with 10% HCl. The aqueous solution was extracted with EtOAc, and the organic layer was dried over $Na_2SO_4$ and concentrated under reduced pressure to afford **19** (345 mg, 40%) as a white solid: mp 131−132 °C (dec); IR (powder) $cm^{-1}$ 3500−3200, 3150−2990, 1701, 1533; $^1H$ NMR (400 MHz, DMSO-$d_6$) $\delta$ 7.86 (d, $J$ = 7.7 Hz, 4H), 7.65 (d, $J$ = 7.5 Hz, 4H), 7.39 (t, $J$ = 7.5 Hz, 4H), 7.29 (t, $J$ = 7.3 Hz, 4H), 7.18 (br, 2H), 4.27 (d, $J$ = 6.7 Hz, 4H), 4.20−4.18 (m, 2H), 3.06−3.05 (m, 4H), 2.67−2.66 (m, 2H); $^{13}C$ NMR (100 MHz, DMSO-$d_6$) $\delta$ 157.1, 143.8, 141.3, 127.7, 127.0, 125.0, 120.0, 66.7, 62.2, 47.2, 43.4; HRMS (ESI) *m/z* calcd for $C_{36}H_{36}N_3O_6$ 606.2599 ([M + H]$^+$), found 606.2601.

**Solid-Phase Synthesis. Loading of 18 onto the Resin (11) as a General Procedure.** Under argon, to the stirred solution of **18** (289 mg, 0.75 mmol) in $CH_2Cl_2$ (4 mL) was added DIPEA (0.52 mL, 3 mmol), 2-chlorotrityl chloride resin (1−1.5 mmol/g, 500 mg, 0.5−0.75 mmol) at room temperature. After 3 h, the reaction solvent was removed by filtration. The remaining resin was washed with $CH_2Cl_2$/MeOH/DIPEA (17/2/1, 4 mL), $CH_2Cl_2$ (4 mL), DMF (4 mL), $CH_2Cl_2$ (4 mL), three times each, and dried under reduced pressure to afford the resin loading **18** (0.86 mmol/g) as pale yellow resin. A mixture of the above resin and piperidine (0.8 mL) was shaken in DMF (3.2 mL) for 30 min at room temperature, and the solvents were removed by filtration. The remaining resin was washed three times each with NMP (4 mL) and $CH_2Cl_2$ (4 mL) and dried under reduced pressure to afford the amino-containing resin **11** as a pale yellow resin. Unreacted chlorotrityl groups were blocked by using hexylamine/THF (1/6, 1.2 mL), and the resin was washed and dried in the same way as above.

**Resin (8) and (14).** The resins **8** and **14** were prepared from 2-chlorotrityl chloride resin with the use of Fmoc-$\beta$-alanine or **18**, respectively, by a similar method as described above.

**General Procedure of Coupling with 18 on Resin.** To a solution of the **18** (5 equiv to the resin) in NMP (1 mL) was added the resin, DIPEA (10 equiv to the resin), and a solution of HBT (10 equiv to the resin) and HBTU (10 equiv to the resin) in DMF (1 mL) at room temperature. The mixture was shaken at room temperature for 2 h. The reaction solvents were removed by filtration. The remaining resin was washed three times each with NMP (3 mL) and $CH_2Cl_2$ (3 mL) and dried under reduced pressure to afford the corresponding *N*-Fmoc-containing resin. The reaction was monitored by checking the residual amino group with use of ninhydrin. A mixture of the above resin and piperidine (0.8 mL) in DMF (3.2 mL) was shaken for 30 min at room temperature. The reaction solvent was removed by filtration. The remaining resin was washed three times each with NMP (4 mL) and $CH_2Cl_2$ (4 mL) and dried under reduced pressure to afford the corresponding resin containing the expanded linker with the amino terminal as a pale yellow resin.

**General Procedure of Coupling with Hoechst-COOH (7) on Resin**. A mixture of the resin and Hoechst-COOH (**7**) (0.5 equiv to the resin), DIPEA (5 equiv to the resin), HBT (5 equiv to the resin), and BOP (5 equiv to the resin) in DMF/NMP (0.5 mL/0.5 mL) was shaken at room temperature for 5 h. The reaction solvents were removed by filtration. The remaining resin was washed three times each with NMP (3 mL) and $CH_2Cl_2$ (3 mL) and dried under reduced pressure.

**Synthesis of Branched Linker on Resin (16).** The resin **14** was subjected to elongation of the linker with use of **18** two times to give the linker-elongated resin. A mixture of the above resin, **19** (10 equiv to the resin), DIPEA (10 equiv to the resin), HBT (10 equiv to the resin) and HBTU (10 equiv to the resin) in DMF/NMP (1 mL/2 mL) was shaken at room temperature for 15 h. The reaction solvents were removed by filtration. The remaining resin was washed three times each with NMP (3 mL) and $CH_2Cl_2$ (3 mL) and dried under reduced pressure. The unreacted amino residue was capped by using benzoic anhydride (10 equiv to the resin), DIPEA (10 equiv to the resin) in $CH_2Cl_2$ (4 mL), and the resin was washed and dried under reduced pressure. The above resin was shaken in DMF (3.2 mL) containing piperidine (0.8 mL) at room temperature for 30 min. The reaction solvents were removed by filtration. The remaining resin was washed and dried under reduced pressure to afford the diaminolinker-containing resin (**16**) as pale yellow resin.

**Coupling of Linker-Containing Hoechst Intermediates (10, 12, and 13) with Diaminolinker-Containing Resin (16).** A mixture of the diamino-resin **16**, the linker-containing Hoechst intermediates (**10**, **12**, or **13**) (4−25 equiv to **16**), DIPEA (4−25 equiv to **16**), and a solution of HBT (25 equiv to **16**) and HBTU (4−25 equiv to **16**) in DMF/NMP (0.75 mL/0.75 mL) was shaken at room temperature for 20 h. The reaction solvents were removed by filtration. The remaining resin was washed three times each with NMP (3 mL) and $CH_2Cl_2$ (3 mL) and dried under reduced pressure to afford the corresponding coupled product.

**Cleavage and Purification of Linker-Bearing Hoechst Derivatives (1, 10, 12, and 13).** The Hoechst-containing resin was treated with 10% TFA in $CH_2Cl_2$ (4 mL) in a 10 mL glass vial for 90 min at room temperature. The mixture was filtered and the remaining resin was washed with THF (3 mL). The combined filtrates were concentrated under reduced pressure. The crude product was purified by reverse-phase HPLC (nacalai tesque COSMOSIL 5C18-AR-II 10 mm × 250 mm; eluents; 0.5% (v/v) TFA in $H_2O$ (A) and 0.5% (v/v) TFA in acetonitrile (B); gradient 0−20 min, 10−40% B in A + B; flow rate 4 mL/min; detection 254 nm) to afford the Hoechst ligand. (8.68 $\mu$mol, 20%) as a yellow solid. Overall yield was determined by quantitative measurement of $^1H$ NMR in DMSO-$d_6$ with 4 mM maleic acid as an internal standard.

**Hoechst Intermediate 10.** The Hoechst intermediate **10** was obtained from the resin **9** (50 mg, 63 $\mu$mol) and Hoechst-COOH (**7**) (14.6 mg, 31 $\mu$mol) as a yellow solid (9.3 $\mu$mol, 30%): IR (powder) $cm^{-1}$ 3100−2800, 1667, 1464, 1429, 1298, 1187, 1114; $^1H$ NMR (400 MHz, MeOH-$d_4$) $\delta$ 8.50 (s, 1H), 8.36 (d, $J$ = 8.6 Hz, 1H), 8.05 (d, $J$ = 8.8 Hz, 2H), 7.88 (d, $J$ = 8.6 Hz, 1H), 7.74 (d, $J$ = 2.2 Hz, 1H), 7.36 (d, $J$ = 2.4 Hz, 1H), 7.09 (d, $J$ = 8.6 Hz, 2H), 3.83−3.77 (m, 12H), 3.71−3.74 (m, 4H), 3.35−3.34 (m, 2H), 3.23 (t, $J$ = 7.0 Hz, 2H), 3.01 (s, 3H), 2.33 (t, $J$ = 6.9 Hz, 2H); HRMS (ESI) *m/z* calcd for $C_{35}H_{41}N_8O_7$ 685.3093 ([M + H]$^+$), found 685.3044.

**Hoechst Intermediate 12.** The Hoechst intermediate **12** was obtained from the resin **11** (50 mg, 43 $\mu$mol) and Hoechst-COOH (**7**) (10.1 mg, 22 $\mu$mol) as a yellow solid (7.6 $\mu$mol, 35%): IR (powder) $cm^{-1}$ 3100−2800, 1669, 1463, 1429, 1300, 1191, 1114; $^1H$ NMR (400 MHz, MeOH-$d_4$) $\delta$ 8.43 (s, 1H), 8.32 (d, $J$ = 8.6

(37) More, J. D.; Finney, N. S. *Org. Lett.* **2002**, *4*, 3001−3003.

Hz, 1H), 8.02 (d, $J$ = 8.8 Hz, 2H), 7.84 (d, $J$ = 8.5 Hz, 1H), 7.70 (d, $J$ = 2.1 Hz, 1H), 7.32 (d, $J$ = 2.1 Hz, 1H), 7.07 (d, $J$ = 8.6 Hz, 2H), 4.04 (s, 2H), 3.87 (s, 2H), 3.84−3.78 (m, 8H), 3.73−3.66 (m, 4H), 3.58−3.56 (m, 2H), 3.49−3.46 (m, 2H), 3.36−3.33 (m, 4H), 3.17 (t, $J$ = 5.7 Hz, 4H), 3.00 (s, 3H); HRMS (ESI) *m*/*z* calcd for $C_{38}H_{47}N_8O_9$ 759.3461 ($[M + H]^+$), found 759.3506.

**Hoechst Intermediate 13.** The Hoechst intermediate **13** was obtained from the resin **11** (100 mg, 86 $\mu$mol) and Hoechst-COOH (**7**) (20.1 mg, 43 $\mu$mol) as a yellow solid (8.7 $\mu$mol, 20%): IR (powder) $cm^{-1}$ 3100−2800, 1663, 1470, 1429, 1298, 1198, 1130; $^1$H NMR (400 MHz, MeOH-$d_4$) $\delta$ 8.51 (s, 1H), 8.38 (d, $J$ = 8.5 Hz, 1H), 8.06 (d, $J$ = 8.8 Hz, 2H), 7.90 (d, $J$ = 8.5 Hz, 1H), 7.76 (d, $J$ = 2.1 Hz, 1H), 7.36 (d, $J$ = 2.1 Hz, 1H), 7.10 (d, $J$ = 8.8 Hz, 2H), 4.07 (s, 2H), 3.89 (s, 2H), 3.88 (s, 2H), 3.84−3.78 (m, 6H), 3.73−3.72 (m, 2H), 3.64−3.62 (m, 2H), 3.58−3.53 (m, 6H), 3.49−3.48 (m, 6H), 3.39−3.34 (m, 6H), 3.20 (t, $J$ = 5.6 Hz, 4H), 3.02 (s, 3H); HRMS (ESI) *m*/*z* calcd for $C_{44}H_{59}N_9O_{12}$ 452.7136 ($[M + 2H]^{2+}$), found 452.7126; MALDI-TOF MS *m*/*z* calcd for ($[M + Na]^+$) $C_{44}H_{57}N_9O_{12}Na$ 927.0, found 926.2.

**Monomer Hoechst Ligand (15).** The monomer Hoechst ligand (**15**) was obtained from the diaminoether-containing resin (**14**) (0.4 mmol/g, 100 mg, 0.04 mmol) and Hoechst-COOH (**7**) (18.7 mg, 0.04 mmol) as a yellow solid (8.78 $\mu$mol, 22%): $^1$H NMR (500 MHz, MeOH-$d_4$) $\delta$ 8.51 (s, 1H), 8.38 (d, $J$ = 8.5 Hz, 1H), 8.06 (d, $J$ = 8.8 Hz, 2H), 7.90 (d, $J$ = 8.5 Hz, 1H), 7.77 (d, $J$ = 2.4 Hz, 1H), 7.37 (d, $J$ = 2.1 Hz, 1H), 7.10 (d, $J$ = 8.8 Hz, 2H) 3.97 (s, 2H), 3.96 (s, 2H), 3.92 (s, 2H), 3.89 (s, 2H), 3.84−3.79 (m, 6H), 3.74−3.72 (m, 4H), 3.70−3.61 (m, 14H), 3.57−3.52 (m, 12H), 3.48−3.38 (m, 8H), 3.25−3.22 (m, 4H), 3.20−3.11 (m, 4H), 3.01 (s, 3H); HRMS (ESI) *m*/*z* calcd for $C_{56}H_{84}N_{12}O_{16}$ 590.3056 ($[M + 2H]^{2+}$), found 590.3025; MALDI-TOF MS *m*/*z* calcd for $C_{56}H_{83}N_{12}O_{16}$ 1180.3 ($[M + H]^+$), found 1180.9.

**Short Bis-Hoechst (1S; *m,n* = 1,1).** Short Bis-Hoechst was obtained from the branched resin (**16**) (40 mg, 16.3 $\mu$mol) and Hoechst intermediate **11** (65 $\mu$mol) as a yellow solid (0.084 $\mu$mol, 1%): $^1$H NMR (500 MHz, MeOH-$d_4$) $\delta$ 8.17 (s, 2H), 8.04 (d, $J$ = 8.2 Hz, 2H), 7.89 (d, $J$ = 8.7 Hz, 4H), 7.60 (d, $J$ = 8.5 Hz, 2H), 7.58−7.57 (m, 2H), 7.19−7.18 (m, 2H), 6.94 (d, $J$ = 8.7 Hz, 4H), 3.96 (s, 2H), 3.93 (s, 2H), 3.90 (s, 4H), 3.86−3.81 (m, 16H), 3.75−3.74 (m, 4H), 3.69−3.34 (m, 49H), 3.20 (t, 4H, $J$ = 6.9 Hz), 3.16−3.15 (m, 2H), 3.00 (s, 6H), 2.29 (t, $J$ = 6.9 Hz, 4H); HRMS (ESI) *m*/*z* calcd for $C_{94}H_{131}N_{23}O_{21}$ 479.4967 ($[M + 4H]^{4+}$), found 479.4933; MALDI-TOF MS *m*/*z* calcd for ($[M + H]^+$) $C_{94}H_{128}N_{23}O_{21}$ 1916.2, found 1915.4.

**Middle Bis-Hoechst (1M; *m,n* = 0,2).** Middle Bis-Hoechst was obtained from the branched resin (**16**) (50 mg, 20 $\mu$mol) and Hoechst intermediate **12** (485 $\mu$mol) as a yellow solid (0.8 $\mu$mol, 4%): $^1$H NMR (500 MHz, MeOH-$d_4$) $\delta$ 8.25 (s, 2H), 8.10 (d, $J$ = 7.8 Hz, 2H), 7.93 (d, $J$ = 8.7 Hz, 4H), 7.66 (d, $J$ = 8.0 Hz, 2H), 7.64−7.62 (m, 2H), 7.24−7.22 (m, 2H), 6.96 (d, $J$ = 8.5 Hz, 4H), 3.96 (s, 2H), 3.94 (s, 2H), 3.91 (s, 4H), 3.89 (s, 4H), 3.86−3.76 (m, 12H), 3.67−3.66 (m, 4H), 3.63−3.36 (m, 54H), 3.23−3.16 (m, 8H), 3.11−3.09 (m, 8H), 3.00 (s, 6H); HRMS (ESI) *m*/*z* calcd for $C_{100}H_{143}N_{23}O_{25}$ 516.5151 ($[M + 4H]^{4+}$), found 516.5191; MALDI-TOF MS *m*/*z* calcd for $C_{100}H_{139}N_{23}O_{25}$ 2063.3 ($[M + H]^+$), found 2062.3.

**Long Bis-Hoechst (1L; *m,n* = 0,3).** Long Bis-Hoechst was obtained from the branched resin (**16**) (100 mg, 40 $\mu$mol) and Hoechst intermediate **13** (183 $\mu$mol) as a yellow solid (1.95 $\mu$mol, 5%): $^1$H NMR (400 MHz, MeOH-$d_4$); $\delta$ 8.33 (s, 2H), 8.24 (d, $J$ = 8.5 Hz, 2H), 7.97 (d, $J$ = 8.5 Hz, 4H), 7.76 (d, $J$ = 8.2 Hz, 2H), 7.64−7.63 (m, 2H), 7.27−7.26 (m, 2H), 7.02 (d, $J$ = 8.2 Hz, 4H), 3.98−3.97 (m, 8H), 3.90−3.89 (m, 8H), 3.86−3.81 (m, 16H), 3.75−3.74 (m, 4H), 3.69−3.49 (m, 55H), 3.44−3.34 (m, 16H), 3.25−3.23 (m, 8H), 3.20−3.12 (m, 4H), 3.00 (s, 6H); HRMS (ESI) *m*/*z* calcd for $C_{112}H_{165}N_{25}O_{31}$ 589.0520 ($[M + 4H]^{4+}$), found 589.0514; MALDI-TOF MS *m*/*z* calcd for $C_{112}H_{162}N_{25}O_{31}$ 2354.6 ($[M + H]^+$), found 2352.7.

**SPR Measurement. Loading of Hoechst Ligand onto a Sensor Chip.** The ligand was dissolved in acetate buffer (pH 4.5, 10 $\mu$M) and immobilized on a sensor chip CM5 (carboxymethylated dextran surface) using an amine coupling kit in HBS-N running buffer (0.01 M HEPES, 0.15 M NaCl, pH 7.4) at 25 °C. The amount of the ligand immobilized on the surface was monitored as an increase of the SPR signal. The density of the immobilized ligand on the surface was calculated by the difference in SPR response before and after immobilization, in which SPR response of 1000 RU is equivalent to the change in surface concentration of 1 ng/mm$^2$. One flow channel was always left as a blank for reference. The remaining carboxyl groups on the sensor surface were quenched with 35 $\mu$L of 1 M ethanolamine, pH 8.5 with flow rate of 10 $\mu$L/min.

**Procedure of SPR Binding Experiments.** Prior to binding experiments, DNA sample in a buffer was annealed by slow cool-down to room temperature after heating at 80 °C for 3 min. SPR measurement was performed in NBS-N running buffer at 25 °C Binding was measured at 20 $\mu$L/min for 120 s and dissociation for 150 s. DNA samples bound on the sensor surface were removed following each measurement by using glycine-NaOH buffer (pH 1.5) as regeneration solution at 30 $\mu$L/min for 30 s.

**Acknowledgment.** This work has been supported by a Grant-in-Aid for Scientific Research (A) from Japan Society for the Promotion of Science (JSPS), and CREST from Japan Science and Technology Agency (JST).

**Supporting Information Available:** $^1$H NMR and MS spectra of Hoechst analogues in Schemes 1 and 2. This material is available free of charge via the Internet at http://pubs.acs.org.

JO051836T